Competitive photodissociation channels in jet-cooled HNCO: Thermochemistry and near-threshold predissociation

M. Zyrianov, Th. Droz-Georget, A. Sanov, and H. Reisler
*Department of Chemistry, University of Southern California, Los Angeles, California 90089-0482*

The photoinitiated unimolecular decomposition of jet-cooled HNCO has been studied following $S_1({}^1A'') \leftarrow S_0({}^1A')$ excitation near the thresholds of the spin-allowed dissociation channels: (1) H $({}^2S)+NCO(X\,{}^2\Pi)$ and (2) $NH(a\,{}^1\Delta)+CO(X\,{}^1\Sigma^+)$, which are separated by 4470 cm^{-1}. Photofragment yield spectra of $NCO(X\,{}^2\Pi)$ and NH $(a\,{}^1\Delta)$ were obtained in selected regions in the 260–220 nm photolysis range. The $NCO(X\,{}^2\Pi)$ yield rises abruptly at 38 380 cm^{-1} and the spectrum exhibits structures as narrow as 0.8 cm^{-1} near the threshold. The linewidths increase only slowly with photolysis energy. The jet-cooled absorption spectrum near the channel (1) threshold $[D_0(H+NCO)]$ was obtained using two-photon excitation via the S_1 state, terminating in a fluorescent product. The absorption spectrum is similar to the NCO yield spectrum, and its intensity does not diminish noticeably above $D_0(H+NCO)$, indicating that dissociation near threshold is slow. The NCO product near threshold is cold, as is typical of a barrierless reaction. NH $(a\,{}^1\Delta)$ products appear first at 42 840 cm^{-1}, but their yield is initially very small, as evidenced also by the insignificant decrease in the NCO yield in the threshold region of channel (2). The NH $(a\,{}^1\Delta)$ yield increases faster at higher photolysis energies and the linewidths increase as well. At the channel (2) threshold, the NH $(a\,{}^1\Delta)$ product is generated only in the lowest rotational level, $J=2$, and rotational excitation increases with photolysis energy. We propose that in the range 260–230 nm, HNCO (S_1) undergoes radiationless decay terminating in S_0/T_1 followed by unimolecular reaction. Decompositions via channels (1) and (2) proceed without significant exit channel barriers. At wavelengths shorter than 230 nm, the participation of an additional, direct pathway cannot be ruled out. The jet-cooled photofragment yield spectra allow the determination, with good accuracy, of thermochemical values relevant to HNCO decomposition. The following heats of formation are recommended: $\Delta H_f^0(HNCO)=-27.8\pm0.4$ kcal/mol, and $\Delta H_f^0(NCO)=30.3\pm0.4$ kcal/mol. These results are in excellent agreement with recent determinations using different experimental techniques. © *1996 American Institute of Physics.* [S0021-9606(96)02941-8]

I. INTRODUCTION

Isocyanic acid, HNCO, is implicated in the removal of NOx products in a process known in combustion as RAPRENOx (rapid reduction of NOx), in energetic materials combustion, and in interstellar space. Therefore, the mechanisms of its decomposition and chemical reactions are of interest. Although much work has been done on the UV photodissociation of HNCO,[1–7] little is known about the mechanism of its decomposition following excitation to the $S_1({}^1A'')$ state near the respective thresholds for the two spin-allowed channels:

$$HNCO \rightarrow H({}^2S)+NCO(X\,{}^2\Pi), \quad (1)$$

$$\rightarrow NH(a\,{}^1\Delta)+CO(X\,{}^1\Sigma^+). \quad (2)$$
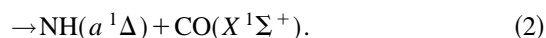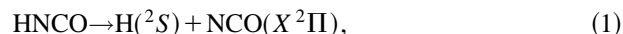
This state of affairs is partly a result of uncertainties regarding the threshold energies for reactions (1) and (2).

Dixon and Kirby have reported that the weak UV absorption of HNCO at 300 K reaches a plateau around 200 nm with a tail extending to ~280 nm.[8] At the tail, the vibronic bands have a well-defined rotational structure, and the perpendicular nature of the $S_1({}^1A'') \leftarrow S_0({}^1A')$ transition, as well as the rotational structure of some of the bands, have been determined. Note that HNCO undergoes substantial bending of the NCO skeleton upon excitation—from 172° in the ground state to 120–130° in the excited state. This severe

change in geometry accounts for the pronounced Franck–Condon activity in the NCO bend, and in part for the breadth of the absorption band. Dixon and Kirby note that the spectrum becomes progressively more diffuse at shorter wavelengths, and at <220 nm vibronic structure can no longer be discerned. These results indicate that the S_1 state is bound and that predissociation is likely to be the preferred mechanism following S_1 excitation, at least at low excess energies.

The heat of formation of HNCO and its dissociation thresholds via channels (1) and (2) have been the subject of some controversy.[4,9] A schematic energy diagram is shown in Fig. 1. Recently, Ruscic and Berkowitz,[9] and Zhang et al.,[4] using different experimental techniques, determined the upper bounds to the dissociation energy of channel (1) as 110.1±0.3 and 110.1±0.5 kcal/mol, respectively. Thus, despite earlier controversy, this value appears now well established. The dissociation threshold of channel (2) remains less certain. The most recent measurements were carried out by Chandler and co-workers who preferred a value of 41 530 cm^{-1} (118.7 kcal/mol),[1–3] although a value of 42 700 cm^{-1} (122.0 kcal/mol) can also be deduced from their data (see below). Accurate values of the dissociation thresholds are not only important for establishing the heats of formation of HNCO and the NCO radical, but also for unraveling decomposition mechanisms and their excess energy dependencies.

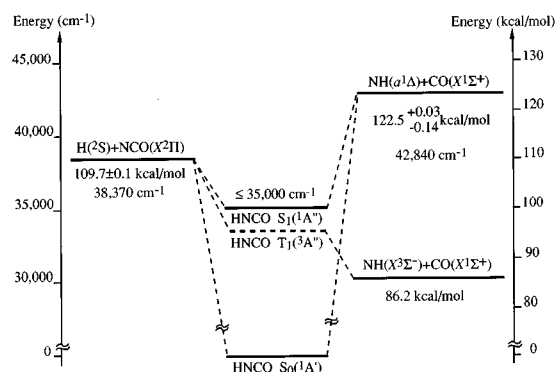For near-threshold studies, expansion cooling of the

FIG. 1. Schematic energy level diagram of the three lowest-energy dissociation channels of HNCO. The thermochemical values are those obtained in this work.

FIG. 2. (a) Two-photon excitation spectrum of jet-cooled HNCO near D_0(H+NCO). Arrows mark the peaks shown on an expanded scale in Fig. 3. (b) NCO photofragment yield spectrum obtained by monitoring the Q_{11} bandhead (low J) of the $(00^00\text{-}00^10)$ $A\,^2\Sigma^+ \leftarrow X\,^2\Pi$ transition. The respective excitation/detection schemes are also shown; see text for details.

sample is beneficial, since the rotational temperature of the parent is low and well defined, and vibrational hot bands are largely suppressed. In this paper we report values for the thresholds of reactions (1) and (2) obtained with jet-cooled samples of HNCO.[10] We confirm and improve the accuracy of the most recent values for channel (1), and determine an upper limit for channel (2) at $42\,840^{+10}_{-60}$ cm^{-1}. In addition, we propose that the decomposition of HNCO proceeds mainly via predissociation on lower electronic surface, rom the onset of channel (1) at 38 370 cm^{-1} (260.6 nm) to at least 43 400 cm^{-1} (230 nm), and that no significant exit channel barriers exist for channels (1) and (2). At higher photolysis energies a direct component to the decomposition cannot be excluded; in fact, previous researches have invoked a fast and direct dissociation mechanism to explain their results.[2–4,11] In addition, Brown *et al.* have recently observed a preference for dissociation via channel (1) relative to channel (2) at a total photolysis energy of 44 400 cm^{-1} (225 nm) when implanting three quanta of NH stretch excitation in HNCO (S_0), as compared with one-photon dissociation at the same energy.[12] This result is hard to rationalize based solely on unimolecular decomposition on S_0.

II. EXPERIMENT

The experimental arrangement used in these pump-probe experiments was described previously.[13] HNCO was prepared and purified following published procedures by the reaction of KOCN with stearic acid.[5] The reagents were heated under vacuum to 90 °C and reaction products were collected in a liquid nitrogen trap. Impurities, mainly CO_2 and water, were removed by trap-to-trap distillation. HNCO was seeded in He or in 30:70 He:Ne mixtures at a typical pressure of 760 Torr by passing the carrier gas through a container with HNCO kept in an acetonitrile/liquid nitrogen bath at -41 °C ($\sim$15-Torr HNCO vapor pressure). The rotational temperature of HNCO in the pulsed jet expansion is estimated at $\sim$10 K (see below). The counterpropagating pump and probe laser beams intersected the molecular beam 5–10 mm (10–20 nozzle diameters) from the nozzle orifice. Both beams were collimated to $\sim$2 mm diameter. The delay between the laser pulses was 50 ns unless varied to deter-
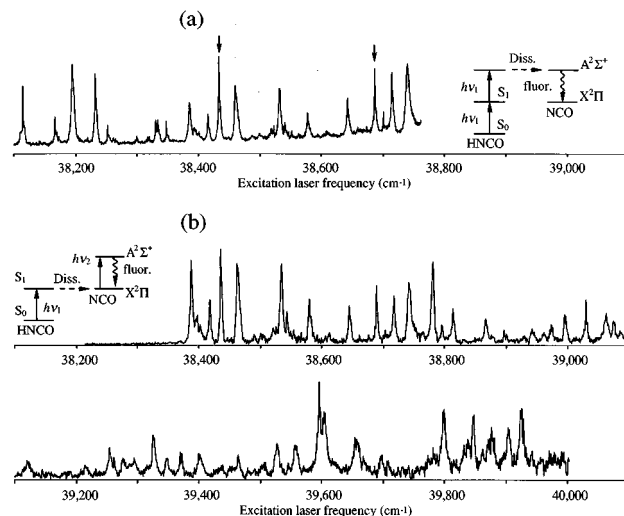
mine the appearance time of the products. HNCO was photolyzed at 260–220 nm using the doubled output of an excimer laser pumped dye laser at typical pulse energies of 1–2 mJ. NCO($X\,^2\Pi$) and NH($a\,^1\Delta$) products were probed by laser induced fluorescence (LIF) via the $A\,^2\Sigma^+ \leftarrow X\,^2\Pi$ and the $c\,^1\Pi \leftarrow a\,^1\Delta$ transitions, respectively,[14,15] using a second excimer laser pumped dye laser (pulse energy $\sim$100–150 μJ). NCO fluorescence in the range 440–500 nm was collected through Kopp 3-72 and 5-60 glass filter, while 0-52 and 7-59 glass filters were used to monitor NH fluorescence at 350–460 nm.

The jet-cooled $S_1 \leftarrow S_0$ absorption spectrum of HNCO was obtained by sequential two-photon excitation via the S_1 state generating electronically excited products. For these studies, the output of the excitation laser was increased to $\sim$3 mJ and focused at the center of the chamber with a 50-cm focal length lens. Quantum yield studies showed that at total excitation energies (one-photon) of 75 000 cm^{-1} the main fluorescing species was NCO ($A\,^2\Sigma^+$).[16] The fluorescence was monitored through Kopp 0-56 and 7-59 filters, which transmitted light at 300–460 nm. Sharp absorption features were obtained whenever the excitation wavelength coincided with an absorption feature of the $S_1 \leftarrow S_0$ transition, both below and above the threshold of channel (1).

III. RESULTS

A. H(^2S)+NCO($X\,^2\Pi$) channel

A portion of the two-photon $S_1 \leftarrow S_0$ absorption spectrum of jet-cooled HNCO is shown in Fig. 2(a), while the NCO photofragment yield spectrum near the channel (1) threshold, D_0(H–NCO), is shown in Fig. 2(b). The Q_{11} bandhead of the NCO ($A\,^2\Sigma^+ \leftarrow X\,^2\Pi$) transition (low J's) was monitored. The NCO yield rises abruptly at 38 380 cm^{-1} and the spectrum remains highly structured. Notice that there are no significant changes in the intensities and

widths of the spectral features in the absorption spectrum obtained by sequential two-photon absorption via S_1 when the dissociation threshold is crossed [Fig. 2(a)]. The complete jet-cooled absorption spectrum from the origin of the S_1 state ($\sim35\,000$ cm^{-1}) has been obtained in this manner; assignments are in progress and will be reported separately.[17] No one-photon LIF from HNCO could be detected. The spectral features below D_0(H–NCO), and some above, exhibit rotational structure within our resolution (0.2 cm^{-1}). The rotational line spacings are consistent with a small change in the B rotational constant in S_1 compared to S_0, in accordance with Dixon and Kirby.[8] Simulated rotational contours of C-type bands give a rotational temperature of ~10 K. The small shoulder to the red of the first main peak in the NCO yield spectrum [Fig. 2(b)] results from photolysis of parent molecules with some rotational excitation.

The NCO($X\,^2\Pi$) product obtained near D_0 is cold and the number of populated rotational levels increases with excitation energy. Yet, dissociation at the peak of the first NCO spectral feature (38 387 cm^{-1}) generates NCO with rotational levels up to $J=6.5$, corresponding to a maximum of 20 cm^{-1} in rotational energy. The rotational excitation may derive partly from rotationally excited HNCO in the ~10 K expansion; however, it is more likely due to the fact that no absorption feature exists at the exact dissociation threshold, as can be seen by comparing Figs. 2(a) and 2(b). Taking the rotational excitation of NCO into account we place the dissociation threshold at 38 370$\pm$30 cm^{-1}.

Since spectral features separated by ~0.8 cm^{-1} could be resolved even above D_0(H–NCO), the near-threshold lifetimes of the S_1 state are estimated at $\geqslant6$ ps. This is only a lower bound on the lifetime, since saturation and spectral overlap can broaden the peaks. However, some spectral feature are broader than ~1 cm^{-1}; for example, in Fig. 3 we display an absorption band obtained following photolysis at 60 cm^{-1} above D_0(H–NCO) which does not reveal rotational structure, while in the spectrum obtained at 315 cm^{-1} above D_0(H–NCO) rotational structure can be discerned. Near-threshold time resolved measurements of NCO($X\,^2\Pi$) indicate appearance times <10 ns, limited by the time resolution of our measurement.

B. NH($a\,^1\Delta$)+CO($X\,^1\Sigma^+$) channel

The NH($a\,^1\Delta$) (hereafter referred to as ^{1}NH) yield spectrum is shown in Fig. 4(a). The spectrum was obtained by monitoring the $Q(2)$ line (arising from the lowest rotational level of the $a\,^1\Delta$ state). The overall decrease observed in the yield spectrum above 44 500 cm^{-1} does not signify a drop in the ^{1}NH quantum yield, but is due to a decrease in the fractional population of ^{1}NH $J=2$ with excitation energy. From the average envelope of the yield spectrum and the rotational distributions shown in Fig. 4(b), we estimate an eightfold increase in ^{1}NH yield between 43 320 and 44 500 cm^{-1}. Notice that the yield increases only slowly initially, but then rises more steeply with photolysis energy. The structure in the spectrum is reproducible and includes fairly narrow features even at the highest photolysis energies.
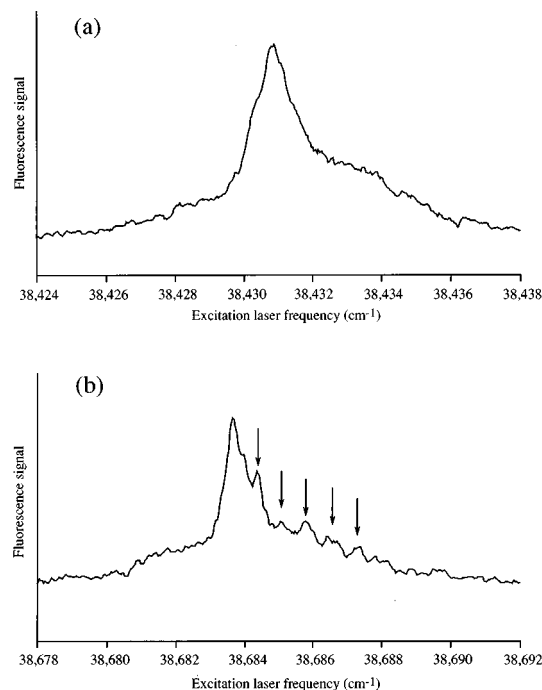

FIG. 3. Two-photon excitation spectra of jet-cooled HNCO recorded at (a) 60 cm^{-1} and (b) 315 cm^{-1} above D_0(H-NCO)=38 370 cm^{-1}. The excitation scheme is shown in Fig. 2(a). Arrows in (b) indicate partially resolved rotational structure; in (a) rotational structure is not observed. The laser bandwidth is 0.2 cm^{-1}.

The first spectra peak that can be confidently assigned to one-photon dissociation via channel (2) is at $\sim42\,900$ cm^{-1}, where only $J=2$ of ^{1}NH is populated. The rotational excitation increases rather monotonically with photolysis energy
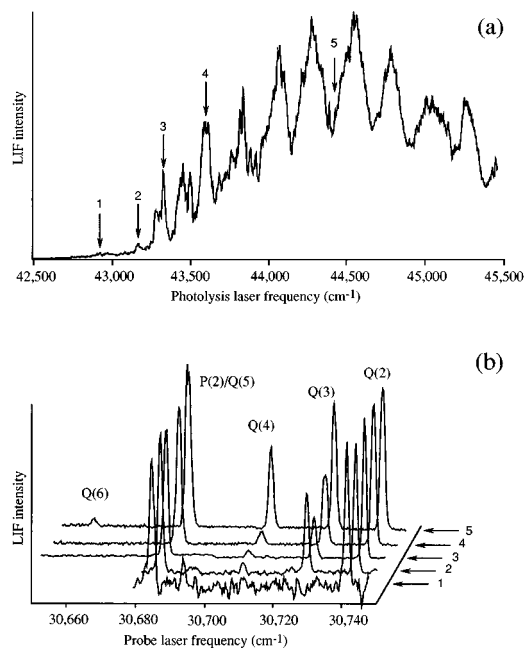

FIG. 4. (a) NH($a\,^1\Delta$)photofragment yield spectrum obtained by monitoring the $Q(2)$ line of the $c\,^1\Pi\leftarrow a\,^1\Delta$ transition. The spectrum is not normalized to the fractional yield of NH in the $J=2$ state. Arrows with numbers indicate excitation energies at which NH rotational distributions were taken. (b) NH ($c\,^1\Pi\leftarrow a\,^1\Delta$)LIF spectra recorded at photolysis energies: (1) 42 900 cm^{-1}; (2) 43 160 cm^{-1}; (3) 43 320 cm^{-1}; (4) 43 600 cm^{-1}; (5) 44 500 cm^{-1}.
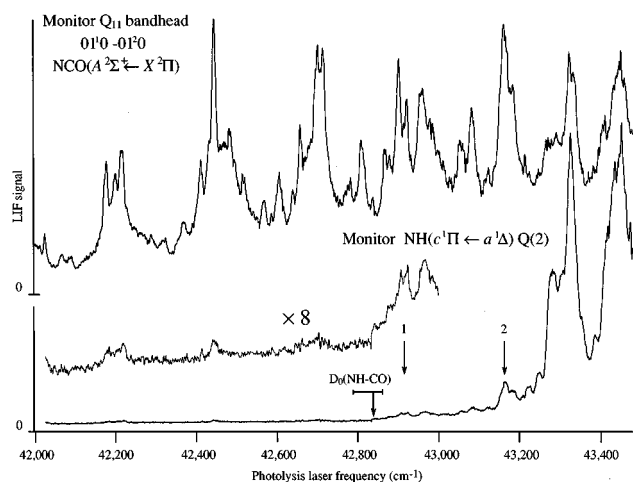
FIG. 5. NCO($X\,^2\Pi$) and NH($a\,^1\Delta$) photofragment yield spectra near D_0(NH+CO). Top trace: NCO ($X\,^2\Pi$) photofragment yield spectrum obtained by monitoring the Q_{11} bandhead of the (01^{1}0-01^{2}0) $A\,^2\Sigma^+\leftarrow X\,^2\Pi$ transition. Bottom trace: NH($a\,^1\Delta$) photofragment yield spectrum obtained by monitoring the $Q(2)$ line of the $c\,^1\Pi\leftarrow a\,^1\Delta$ transition. Middle trace: part of the NH spectrum with intensity multiplied by a factor of 8 to highlight the threshold for one-photon dissociation. The NH and NCO yield spectra are not normalized to each other to reflect their relative quantum yields.

[Fig. 4(b)], although near threshold some irregularities appear; for example, the distribution taken with 43 160-cm^{-1} excitation appears anomalously hot. The NCO and ^{1}NH yield spectra in the region of the onset of channel (2) are displayed in Fig. 5. Here the Q_{11} bandhead of the 010-010 band of the NCO ($A\,^2\Sigma^+\leftarrow X\,^2\Pi$) transition, whose fractional population is nearly constant over this narrow excitation energy range, is monitored.[18] The peak heights within each spectrum reflect the correct relative intensities, but the NCO and ^{1}NH spectra are not normalized to reflect the relative quantum yields of channels (1) and (2). Notice that the yield of NCO does not drop significantly with the opening of channel (2), and the NCO and ^{1}NH spectra exhibit the same structure. Figure 5 shows an expanded trace of the ^{1}NH yield spectrum in the threshold region, where very small peaks (similar to features in the NCO yield spectrum) are observed even below the 42 900-cm^{-1} peak. These peaks appear only at the high laser fluences required to see the small threshold spectral feature, and their intensities do not diminish at lower excitation energies; they are therefore ascribed to two-photon dissociation, a rather efficient process even above dissociation threshold.

Preliminary results of photofragment ion imaging experiments in which H/D fragments are produced by one-color photodissociation/detection of jet-cooled H(D)NCO at 243.1 nm (41 129 cm^{-1}) do not reveal significant anisotropy in the photofragment recoil, supporting relatively slow dissociation. At shorter wavelengths, β recoil anisotropy parameters of -0.7 at 217 nm (46 000 cm^{-1})[11] and -0.85 at 193.3 nm (51 700 cm^{-1})[4] for the CO and H products, respectively, were obtained, indicating much faster dissociation.

IV. DISCUSSION

A. Thermochemical implications

The jet-cooled product yield spectra and state distributions allow us to determine or verify thermochemical data with good accuracy. After correction for rotational excitation in the NCO photofragment, we obtain D_0(H–NCO) $=38\,370\pm30$ cm^{-1} (109.7$\pm$0.1 kcal/mol). This value is slightly lower than, but in excellent agreement with, the values of $\leq110.1\pm0.5$ kcal/mol obtained by Zhang *et al.*[4] and $\leq110.1\pm0.3$ kcal/mol by Ruscic *et al.*,[9] as well as with the recent results of Brown *et al.* (38 320$\pm$140 cm^{-1}; 109.6$\pm$0.4 kcal/mol).[19] The heat of formation of HNCO calculated using ΔH_f^0(H)$=51.63$ kcal/mol (Ref. 20) and ΔH_f^0(NCO)$=30.4\pm1.0$ kcal/mol (Ref. 21) is -27.7 ± 1.0 kcal/mol, limited mainly by the accuracy of the NCO value.

The appearance threshold of channel (2) has been more controversial. We place the threshold at $42\,840^{+10}_{-60}$ cm^{-1}, ($122.5^{+0.03}_{-0.17}$ kcal/mol) with no or a very small barrier. The upper limit is determined by the uncertainty in wavelength calibration and the possibility of excitation of hot rotational bands. The lower limit is determined by the fact that no ^{1}NH signal is observed at 42 800 cm^{-1}, while a peak appears in the NCO yield spectrum at this location (Fig. 5). The value of 114 kcal/mol calculated from Okabe's UV absorption data[22] was increased by Spiglanin *et al.* to 118.7 kcal/mol (41 530 cm^{-1}).[1–3] This value was obtained from their ^{1}NH yield spectra recorded at 300 K after correction for thermal excitation. However, these authors also noted that the average ^{1}NH rotational excitation decreased linearly with photolysis energy in the region from 53 000 cm^{-1} to $\sim$43 000 cm^{-1}, but then leveled off. A straight line extrapolation of their data to zero average ^{1}NH rotational energy (Fig. 4 of Ref. 2) yields a threshold of 42 700$\pm$200 cm^{-1}, in good agreement with our measurements. We believe that this latter method of estimating dissociation thresholds from 300 K data is superior. The recent value obtained by Brown *et al.* with 300-K samples,[19] 42 710$\pm$100 cm^{-1}, also supports the new value. Note that our value is also in excellent agreement with the threshold calculated using ΔH_f^0(HNCO) $=-27.7\pm1.0$ kcal/mol, ΔH_f^0(NH)$=85.6\pm0.3$ kcal/mol,[23] ΔH_f^0(CO) $=-27.20\pm0.04$ kcal/mol,[20] and NH singlet–triplet separation of 36.28 kcal/mol,[15] which gives 122.4 $\pm$1.0 kcal/mol.

We can also use the improved thermochemical data obtained in this work to determine more accurately the heat of formation of NCO. From D_0(^{1}NH–CO) and the ^{1}NH and CO heats of formation given above, we determine ΔH_f^0(HNCO)$=-27.8\pm0.4$ kcal/mol. This value and D_0(H–NCO)$=109.7\pm0.1$ kcal/mol are then used to determine ΔH_f^0(NCO)$=30.3\pm0.4$ kcal/mol, in excellent agreement with the value obtained by Cyr *et al.* using a different method.[21]

B. Near-threshold decomposition mechanism

The reported jet-cooled absorption and yield spectra, as well as the product state distributions, strongly suggest that HNCO predissociated via channels (1) and (2) without sig-

nificant barriers following radiationless decay to a bound electronic state, most likely S_0. From the widths of the absorption features above D_0(H–NCO), we infer that the S_1 lifetime near D_0 is longer than ~6 ps (but shorter than 10 ns, as obtained from the NCO appearance time). The widths increase only slowly with excitation energy; in fact, the lines remain rather narrow even >1000 cm^{-1} above D_0. Another signature of the slowness of the near-threshold dissociation is obtained from the two-photon absorption spectrum [Fig. 2(a)]: The spectral intensity does not diminish noticeably above D_0(H–NCO), indicating that second photon absorption easily competes with dissociation. This mechanism suggest that the linewidths near threshold reflect the coupling strengths in the radiationless decay step, which are expected to vary only slowly with energy.[24] Had predissociation occurred on S_1 (whose well depth is <4000 cm^{-1}), its rate would have increased much faster, and large state-to-state fluctuations in the widths [as seen for example in the photodissociation of HCO (Ref. 25) and CH$_3$O (Ref. 26)] might also be expected. We do observe some state specificity in the linewidths above D_0(H–NCO). For example, in Fig. 3 the linewidths obtained at excess energy ~60 cm^{-1} above D_0(H–NCO) are broader than those obtained at 315 cm^{-1}. This state specificity most probably originates in the radiationless decay step and is not associated with the dissociation rate on S_0.[24]

Rate calculation of the decomposition using the Rice–Ramsperger–Kassel–Marcus (RRKM) theory support dissociation on S_0 rather than on S_1. Assuming a loose transition state and no barrier to channel (1), we find dissociation rates between D_0 and D_0+1000 cm^{-1} that range from ~10^9 s^{-1} to ~5×10^{11} s^{-1}.[27] At comparable excess energies, decomposition on S_1 would result in rates faster than 10^{12} s^{-1} (corresponding to linewidths >5 cm^{-1}) that increase rapidly with excess energy, which is in contradiction with the experimental observations.

Dissociation via channel (1) is favored to proceed on S_0 rather than on T_1, since recent calculations reveal a substantial barrier to channel (1) on the latter surface.[28] Even at energies above that barrier, dissociation on S_0 is likely to dominate since dissociation on T_1 would be difficult to reconcile with a significant yield of H+NCO when the energetically lowest pathway, NH($X^3\Sigma^-$)+CO, is already open (see Fig. 1).

The S_1/S_0 coupling matrix elements must be small; using the observed linewidth $\Gamma \approx 1$ cm^{-1} and $\rho \approx 10^3$/cm^{-1} (as a rough estimate of the density of states on S_0) in Fermi's golden rule $\Gamma = 2\pi\nu^2\rho$, we obtain that the average coupling matrix element is $\nu \approx 10^{-2}$ cm^{-1}.[24] Another experimental observation supporting weak coupling is the absence of clumps, extra lines, or other manifestations of strong couplings in the $S_1 \leftarrow S_0$ spectrum near the S_1 origin.[17,29] Nevertheless, the absence of detectable fluorescence following S_1 excitation suggests that nonradiative decay of the bright S_1 vibronic states competes favorably with fluorescence. The absence of fluorescence is not surprising, since the $S_1 \leftarrow S_0$ transition is weak (it is equivalent to the forbidden $A\,^1\Sigma_u^- \leftarrow X\,^1\Sigma_g^+$ transition in the isoelectronic CO$_2$, and thus allowed only in

C_s symmetry),[9,22] and its radiative lifetime is expected to be long. Consequently, radiationless decay must be efficient, and a barrier to dissociation via channel (1) on S_1 must exist.

The subsequent dissociation on S_0 proceeds with no significant barrier as suggested by the low rotational excitation of the NCO fragment. With 38 387-cm^{-1} photolysis (the first peak in the NCO yield spectrum), the average rotational energy in the NCO product is only ~10 cm^{-1}, and the next absorption feature to the red of this peak is ~35 cm^{-1} away.

Establishing the dissociation mechanism at wavelengths where both channels (1) and (2) are open is less straightforward. The rotational distributions of the ^{1}NH fragment [Fig. 4(b)] show that only the lowest rotational level, $J=2$, is populated when exciting in the 42 900-cm^{-1} threshold band. Higher rotational levels are populated in turn as the excess energy increases. Again, this behavior is typical of dissociation without a significant barrier. Indeed, quenching experiments of ^{1}NH by CO indicate that no barrier exists in the approach of the two fragments,[30] and recent electronic structure calculations show no barrier on S_0, but barriers on S_1 and T_1.[31] The absence of barrier on S_0 has been rationalized by a change in hybridization as CO approaches ^{1}NH. By analogy with the isoelectronic HN$_3$, barriers on S_1 and T_1 are due to electron–electron repulsion between the in-plane π nonbonding orbital of NH and the σ nonbonding orbital of CO.[32] The electronic configuration of S_0 is more complicated, and in HN$_3$ is best described at long range as excitation of the 10a' orbital whose energy increases as CO and ^{1}NH approach. At closer separation, there is rehybridization to a 2a'' orbital which is attractive. In HN$_3$ this leads to a barrier on S_0; however, in HNCO the S_0 well is much deeper and the barrier is apparently eliminated.[31,32]

The relative quantum yield of ^{1}NH is initially very small; NCO yield spectra taken at the ^{1}NH threshold region show no significant decrease when channel (2) opens (Fig. 5), and Brown *et al.* have very recently estimated that following excitation of 300 K HNCO at 43 480 cm^{-1} the relative ^{1}NH quantum yield Φ_{NH}(230 nm) is <0.03.[12] At higher excess energies, the ^{1}NH relative yield increases. Assuming that for jet-cooled HNCO Φ_{NH}(230 nm)=0.03 as well and ignoring the increase in the average absorption cross section between 230 and 225 nm, we obtain Φ_{NH}(225 nm)≈0.3. Since the branching ratio between channels (1) and (2) depends sensitively on the characteristics of the respective transition states and their dependence on excess energy, it is hard to predict without detailed knowledge of the potential energy surfaces. Nevertheless, assuming that dissociation via both channels proceeds only on S_0, representative RRKM calculations are capable of simulating the observed trends in the branching ratios with physically reasonable parameters for the (rather loose) transition states.[27] Had dissociation to ^{1}NH occurred on S_1 from its onset, the increase in ^{1}NH relative yield and linewidth would have been much faster. Notice that there is no abrupt change in the widths of the spectral features near the threshold for channel (2) mitigating, again, against S_1 participation. At higher excitation energies, the lines progressively broaden and an underlying continuum appears [Fig. 4(a)]. Obviously, this continuum derives partly

from increased spectral congestion, but the participation of a direct channel cannot be ruled out.

V. CONCLUSIONS

The jet-cooled studies presented in this paper enable us to deduce improved thermochemical values relevant to HNCO decomposition. The dissociation thresholds of channels (1) and (2) are $38\,370\pm30$ cm^{-1} (109.7 ± 0.1 kcal/mol) and $42\,840^{+10}_{-60}$ cm^{-1}, ($122.5^{+0.03}_{-0.17}$ kcal/mol), respectively. From these values, we derive improved heats of formation: $\Delta H_f^0(\text{HNCO})=-27.8\pm0.4$ kcal/mol, and $\Delta H_f^0(\text{NCO})=30.3\pm0.4$ kcal/mol. We believe that the thermochemistry of HNCO is now well established.

From the jet-cooled absorption and photofragment yield spectra, as well as the near-threshold $\text{NCO}(X\,^2\Pi)$ and NH $(a\,^1\Delta)$ rotational distributions, we infer the photodissociation mechanism following $S_1 \leftarrow S_0$ excitation. At least up to ~ 5000 cm^{-1} above $D_0(\text{H–NCO})$, radiationless decay accesses high vibrational levels of S_0 from which HNCO predissociates via channels (1) and (2) without significant barriers. This mechanism implies that significant barriers to dissociation must exist on S_1.

Previous product rotational and translational energy distributions following photolysis of 300 K HNCO in the range $41\,000$–$53\,000$ cm^{-1} were interpreted by assuming an impulsive dissociation mechanism on S_1. However, the values for the bond dissociation energies used in the data analyses were incorrect, and in light of the improved thermochemical values now available a reinterpretation of the previous results is recommended. Note also that at 225 nm, Brown *et al.* observe state-specific effects in the vibrationally mediated photodissociation of HNCO, a result that is hard to explain with dissociation proceeding solely on S_0. Thus, at high photolysis energies the mechanism may change. Experiments are currently in progress to compare the product state distributions with statistical theories, and to explore decomposition mechanism(s) at higher photolysis energies.

[1] T. A. Spiglanin, R. A. Perry, and D. W. Chandler, J. Phys. Chem. **90**, 6184 (1986).

[2] T. A. Spiglanin and D. W. Chandler, J. Chem. Phys. **87**, 1577 (1987).

[3] T. A. Spiglanin, R. A. Perry, and D. W. Chandler, J. Chem. Phys. **87**, 1568 (1987); T. A. Spiglanin and D. W. Chandler, Chem. Phys. Lett. **141**, 428 (1987).

[4] J. Zhang, M. Dulligan, and C. Wittig, J. Chem. Phys. **99**, 7446 (1995).

[5] (a) W. S. Drozdoski, A. P. Baronavski, and J. R. McDonald, Chem. Phys. Lett. **64**, 421 (1979); (b) G. T. Fujimoto, M. E. Umstead, and M. C. Lin, Chem. Phys. **65**, 197 (1982).

[6] W. K. Yi and R. Bersohn, Chem. Phys. Lett. **206**, 365 (1993).

[7] B. Bohn and F. Stuhl, J. Phys. Chem.. **97**, 4891 (1993).

[8] R. N. Dixon and G. H. Kirby, Trans. Faraday Soc. **64**, 2002 (1968).

[9] B. Ruscic and J. Berkowitz, J. Chem. Phys. **100**, 4498 (1994).

[10] A preliminary report is given in: M. Zyrianov, A. Sanov, T. Droz-Georget, and H. Reisler, Roy. Soc. Chem. Faraday Disc. **102** (in press).

[11] M. Kawasaki, Y. Sato, K. Suto, Y. Matsumi, and S. H. S. Wilson, Chem. Phys. Lett. **251**, 67 (1996).

[12] S. S. Brown, R. B. Metz, H. L. Berghout, and F. F. Crim (unpublished).

[13] A. Ogai, C. X. W. Qian, and H. Reisler, J. Chem. Phys. **93**, 1107 (1990).

[14] P. S. H. Bolman, J. M. Brown, A. Carrington, I. Kopp, and D. A. Ramsay, Proc. R. Soc. London, Ser. A **343**, 17 (1973).

[15] R. S. Ram and P. F. Bernath, J. Opt. Soc. Am. B **3**, 1170 (1986); C. R. Braizer, R. S. Ram, and P. F. Bernath, J. Mol. Spec. **120**, 381 (1986).

[16] K. Uno, T. Hikida, A. Hiraya, and K. Shobatake, Chem. Phys. Lett. **166**, 475 (1990).

[17] M. Zyrianov, A. Sazonov, R. A. Beaudet, and H. Reisler (unpublished).

[18] S. S. Brown, R. B. Metz, H. L. Berghout, and F. F. Crim, J. Phys. Chem. **100**, 7948 (1996).

[19] S. S. Brown, H. L. Berghout, and F. F. Crim, J. Chem. Phys. **105**, 8103 (1996), preceding paper.

[20] *JANAF Thermochemical Tables*, 3rd ed. (J. Phys. Chem. Ref. Data, 1985).

[21] D. R. Cyr, R. E. Continetti, R. B. Metz, D. L. Osborn, and D. M. Neumark, J. Chem. Phys. **97**, 4937 (1992).

[22] H. Okabe, J. Chem. Phys. **53**, 3507 (1970); *Photochemistry of Small Molecules* (Wiley-Interscience, New York, 1978).

[23] B. Ruscic (private communication). The recommendation to use the above value of $\Delta H_0^f(\text{NH})=85.6\pm0.3$ is based on a combination of the appearance potentials of $\text{NH}_2^+/\text{NH}_3$ and NH^+/NH_2, which are 15.768 ± 0.004 eV and 17.440 ± 0.005 eV, respectively, and $\text{IP}(\text{NH}_2)=11.140\pm0.010$ eV and $\text{IP}(\text{NH})=13.476\pm0.002$ eV, along with $\Delta H_f^0(\text{NH}_3)=-9.31\pm0.008$ kcal/mol. A slightly different value, $\Delta H_f^0(\text{NH})=85.3\pm0.2$ kcal/mol, was recommended by Anderson [W. R. Anderson, J. Phys. Chem. **93**, 530 (1989)].

[24] E. S. Medvedev and V. I. Osherov, *Radiationless Transitions of Polyatomic Molecules* (Springer-Verlag, Berlin, 1995).

[25] S. Williams, J. D. Tobiason, J. R. Dunlop, and E. A. Rohlfing, J. Chem. Phys. **102**, 8342 (1995); J. D. Tobiason, J. R. Dunlop, and E. A. Rohlfing, J. Chem. Phys. **103**, 1448 (1995); D. W. Neyer, X. Luo, P. L. Houston, and I. Burak, J. Chem. Phys. **98**, 5095 (1993); ibid. **102**, 1645 (1995).

[26] A. Geers, J. Kappert, F. Temps, and J. W. Weibrecht, J. Chem. Phys. **93**, 1472 (1990); **98**, 4297 (1993); **99**, 2271 (1993); **101**, 3618, 3634 (1994).

[27] In these simulations the H–NCO transition state frequencies were assumed to include those of free NCO, i.e., 1290, 2338, 680 cm^{-1} (C–N and C–O stretches and NCO bend, respectively), and two nearly free rotors corresponding to the H-atom motion perpendicular to the reaction coordinate and the angular momentum associated with the nearly degenerate bend of the NCO skeleton (20 cm^{-1} for both). The HN–CO transition state frequencies included the N–H and C–O frequencies (3186 and 2214 cm^{-1}, respectively), while three other degrees of freedom (N–CO and HN–C bends and HN–CO relative rotation) were assumed to be rather loose (50, 20, and 20 cm^{-1}). The harmonic density of states of $\text{HNCO}(S_0)$ near the opening of channel (2) used in the calculations is ~ 600 per cm^{-1}, surely a gross underestimation. However, under the assumption of complete Intramolecular Vibrational Redistribution (IVR) this parameter does not affect the NH/NCO channel ratio, as derived from the RRKM theory.

[28] A. M. Mebel, A. Luna, M. C. Lin, and K. Morokuma, J. Chem. Phys. (in press).

[29] The weak coupling may be a result of the large energy gap between S_0 and S_1 which gives rise to unfavorable Franck–Condon overlap factors.

[30] W. Hack and K. Rathmann, J. Phys. Chem. **94**, 3636 (1990).

[31] W. -H. Fang, X. -Z. You, and Z. Yin, Chem. Phys. Lett. **238**, 236 (1995).

[32] M. H. Alexander, H. -J. Werner, and P. J. Dagdigian, J. Chem. Phys. **89**, 1388 (1989); M. H. Alexander, H. -J. Werner, T. Hemmer, and P. J. Knowles, J. Chem. Phys. **93**, 3307 (1990).